

# Monitoring Requirements of the BaBar Silicon Vertex Tracker

Pat Burchat, David Kirkby  
Stanford University

June 12, 1996  
(Revised July 21, 1996)

## **Abstract**

This document specifies the requirements for many of the monitoring tasks associated with the silicon vertex tracker (SVT). It covers monitoring of background radiation levels for diagnostic and detector-protection purposes, monitoring of the positions of the SVT support cones relative to the B1 magnets for safety and alignment purposes, monitoring of the temperatures of the high-density interconnects (HDI's), the SVT mechanical support, and any temperature-sensitive monitoring components, and monitoring of the humidity level in the interaction region. It does not cover the monitoring of power-supply currents for the SVT detectors and readout electronics. It also does not cover monitoring of parameters in the interaction region directly related to the machine (relative positions of PEP-II magnets, temperatures of machine components, beam positions, vacuum, *etc.*).

# Contents

<b>1</b>	<b>General Requirements</b>	<b>3</b>
<b>2</b>	<b>Radiation Monitoring</b>	<b>7</b>
2.1	Radiation Environment . . . . .	8
2.2	SVT Radiation Hardness . . . . .	16
2.3	Interfaces with Other Systems . . . . .	17
2.4	Performance Requirements . . . . .	19
<b>3</b>	<b>Position Monitoring</b>	<b>21</b>
<b>4</b>	<b>Temperature Monitoring</b>	<b>25</b>
4.1	Mechanical Structure . . . . .	25
4.2	HDI's . . . . .	26
4.3	Temperature-dependent Sensors . . . . .	27
<b>5</b>	<b>Humidity Monitoring</b>	<b>27</b>
<b>6</b>	<b>Schedule</b>	<b>28</b>

# 1 General Requirements

In this section we describe the general mechanical and electrical requirements for the SVT monitoring systems covered in this document. The overall mechanical and electrical requirements for the entire SVT system are described elsewhere [1, 2].

Figure 1 shows a sideview (in the  $y$ - $z$  plane) of the PEP-II interaction region and the SVT. The space available for sensors and readout cables for SVT monitoring is extremely scarce. In the forward and backward regions, an annular volume has been reserved for radiation sensors just under the HDI's for the first layer of silicon sensors at the small end of the support cone, as shown in Figure 2. The size of this volume is about 19.7 mm in  $z$  by 3.6 mm in  $r$ . The space reserved for monitoring the relative positions of the support cones and the B1 magnets is at the large end of the support cones. There is more space available in the backward direction than in the forward direction because of the different support-cone shapes. Figure 3 shows a detail of the more constrained space available in the forward direction. The space available for a temperature sensor on each HDI is approximately  $2 \text{ mm} \times 1 \text{ mm}$ .

Front-end electronics for the SVT detectors are located on 104 (52 on each side) high-density interconnect (HDI) modules mounted on the support cone, as shown in Figure 1. Each HDI is connected to a corresponding “matching card” with a pair of flat Kapton “tail” cables. Shielded twisted-pair cables carry signals and power from the matching cards through the support tube and out of the detector (see Figure 4). Each matching card is connected using 20 conductors for power and 34 for signals. Between the Q1 magnet and the support tube, the combined cables from 6 matching cards must fit within a cross-sectional area of 14.3 mm in  $r$  by 73.7 mm in circumference (about  $176 \text{ mm}^2$  per matching card).

SVT monitoring has been allocated cable space equivalent to an additional 2 HDI's on each side of the interaction point (IP). In addition, two conductors per HDI have been allocated in the SVT cable budget for monitoring HDI temperatures. The radiation monitoring sensors located at the small end of the support cones must be read out with flat Kapton cables equivalent in cross-sectional area to those being used to read out two SVT HDI's. This corresponds to a width of 5.33 mm, and a total thickness of 1.7 mm. The design of the tails used for monitoring can be different from the standard SVT tails.

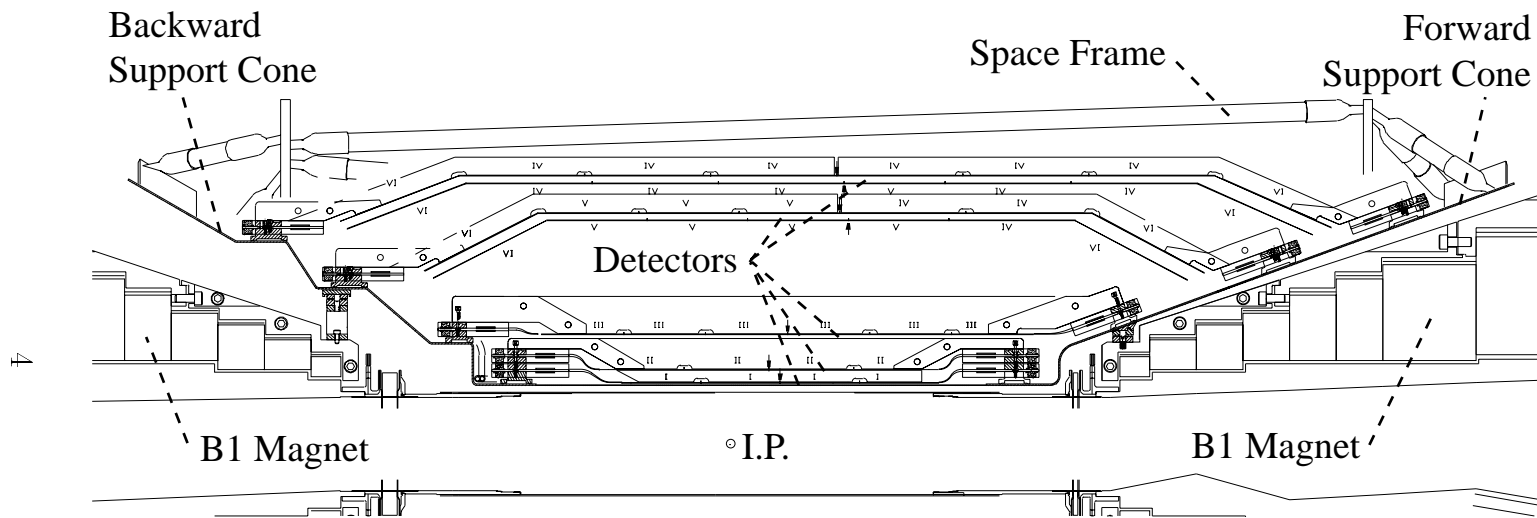


Figure 1: Sideview (in the y-z plane) of the PEP-II interaction region and SVT detector, based on revision K (16 May 96) of CAD drawing B0207a.

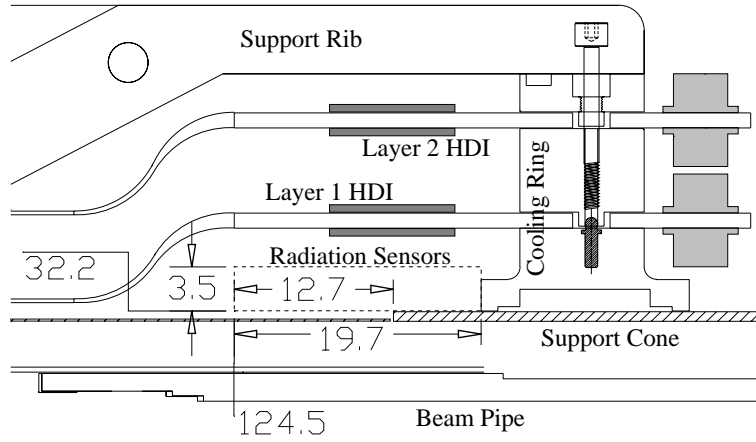


Figure 2: Detail of the space below the first- and second-layer HDI modules, at the small end of the forward support cone. Dimensions are given in millimeters.

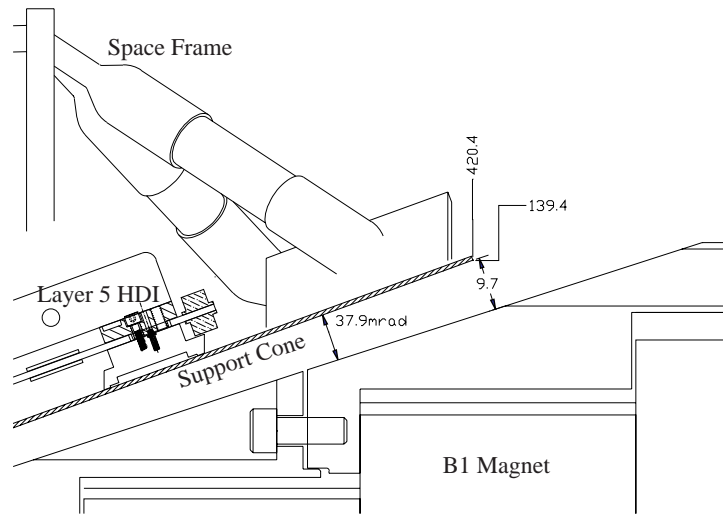


Figure 3: Detail of the space at the large end of the forward support cone. Dimensions are given in millimeters.

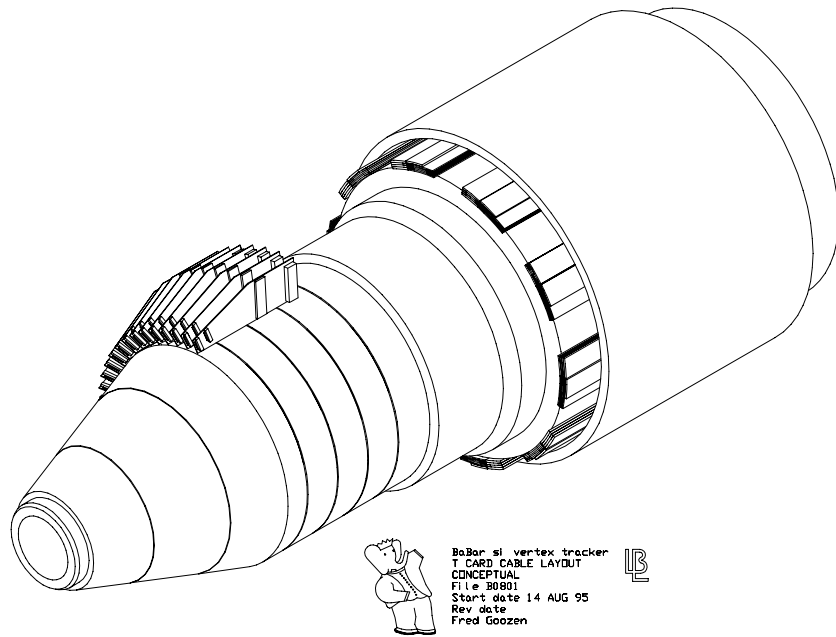


Figure 4: Perspective drawing of one side of the interaction region showing the position of the 54 matching cards around the B1 magnet, and the layout of SVT cable bundles between the support tube and the Q1 magnet.

Position monitors will be located at the large end of each SVT support cone. Since these monitors are so close to the matching cards, it is not necessary to use flat Kapton cables for their readout. Similarly, temperature sensors for the SVT mechanical structure and humidity sensors can be located so that conventional cables can be used to connect them with the monitoring matching cards. All monitoring cables within the support tube should use connectors fixed on one of the 4 matching cards allocated for monitoring (2 on each side). Beyond the matching card, monitoring cables must fit between the support tube and the Q1 magnet, using a space on each side of the IP equivalent to that of two HDI's (i.e., the monitoring cables on each side must pack together with the cables from 4 HDI's to occupy at most  $14.3 \text{ mm} \times 73.7 \text{ mm}$ ).

Possible locations for front-end electronics associated with monitoring sensors are: at the sensor itself, on a monitoring matching card (see Figure 4), in one of the two SVT multiplexer and optical-link racks (located in the interaction hall on either side of the detector, at a cable length of about 7.5 meters), or in the SVT power-supply rack (located in the counting house, at a cable length of about 37.5 meters). The first option is ruled out because of space constraints, except possibly for humidity and temperature sensors located on the space frame. The first two options both require radiation-hard electronics because of the potentially large exposures at these locations. The trade-off for the last two options is between shorter cable lengths (and correspondingly less noise) and better access (only the power-supply rack will be accessible during running).

The design of the SVT electronics, data transmission and power distribution follows shielding and grounding guidelines that minimize noise interference within the SVT and between the SVT and other detector and machine components. SVT monitoring systems should conform to these guidelines, paying particular attention not to degrade the performance of the SVT readout.

## 2 Radiation Monitoring

The primary requirement of this system is to:

- protect SVT components from avoidable radiation damage by early detection of increasing radiation levels and triggering of the PEP-II

beam abort system as well as interlocking of the SVT power-supply system.

The secondary requirements of this system are to:

- provide real-time monitoring of slowly-varying radiation levels in the interaction region for accelerator tuning and diagnostics as well as for SVT power-supply interlocks, and
- to estimate the integrated doses received by SVT detectors and front-end electronics over their lifetime.

The radiation-monitoring system should be operational at all times when beams are present in the accelerator and the SVT is installed. The beam-abort trigger generated by this system should be fully qualified by the accelerator group during accelerator commissioning, before the SVT is installed.

Below, we first describe the expected radiation environment in the interaction region, and then review the radiation hardness and damage mechanisms of the SVT components, as well as the required interfaces of this system with other systems. Finally, we specify the required sensitivity and dynamic range of the radiation monitoring system.

## 2.1 Radiation Environment

The three main modes of PEP-II operation, for the purposes of characterizing radiation levels, are injection (filling or top-up), stable colliding beams, and beam loss (see Figure 5). One complete cycle of machine operation starts with injection to fill the beams (6 minutes), followed by a sequence of one-hour cycles during which beams collide and gradually decay and are then topped-up (3 minutes), and ending with deliberate or accidental dumping of the beams.

SVT backgrounds have been most extensively studied for periods of stable colliding beams. The main sources of background expected during this mode are synchrotron radiation and “lost particles” (see Chapter 12 of Reference [3]). Synchrotron backgrounds are due to kilowatts of low-energy (below 100 keV) photons being produced in the strong bending fields of the accelerator magnets near the IR. Since most of this flux is absorbed in masks designed to shield the detector, synchrotron radiation is not expected to be a major source of radiation exposure for the SVT components (see Table 1). Lost

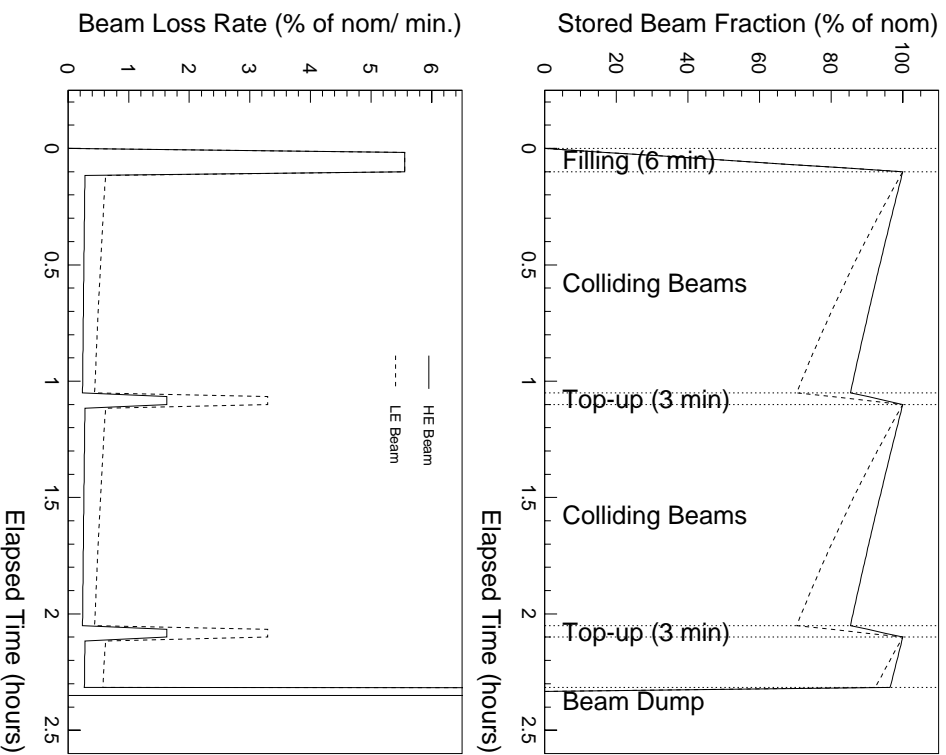


Figure 5: Operating modes of the PEP-II accelerator. The upper plot shows how the stored beam fractions (as percents of nominal full currents) vary during a typical machine cycle. The lower plot shows the corresponding rates of beam loss, expressed as percentage changes of nominal full currents per minute. The plots are calculated assuming beam lifetimes of 6.0 hours (HE beam) and 2.7 hours (LE beam), and an injection efficiency of 75%.

Table 1: Synchrotron radiation background simulation results for periods of stable colliding beams. The first two columns give the expected number of photons and total energy absorbed per bunch crossing (4.202 ns) in each layer for photons with  $4 \text{ keV} < E_\gamma < 100 \text{ keV}$  (see Table 12–2 of Reference [3]). The contribution of photons with energies outside this range is expected to be negligible. The last column gives the dose-rate equivalent to the deposited energy in one crossing ( $1 \text{ yr} \equiv 10^7 \text{ s}$ ).

SVT Layer	number absorbed	energy absorbed	dose rate
1	0.028	430 eV	600 rad/yr
2	0.00069	22 eV	20 rad/yr
3	0.00056	20 eV	10 rad/yr

particles are beam particles that interact with the residual gas present in the beampipe, by bremsstrahlung or Coulomb scattering, and then hit material further downstream, producing an electromagnetic shower of MeV-scale photons and electrons. This background is expected to be the dominant source of radiation exposure for the SVT components during collisions (see Table 2). The loss of beam particles by bremsstrahlung and Coulomb scattering is the main reason for the exponential decay of the beams during collisions shown in Figure 5.

The SVT radiation exposure due to both lost particles and synchrotron radiation is strongly peaked in the horizontal plane but varies more smoothly with  $z$  (see Figures 6 and 7 for lost-particle distributions). Most of the expected dose absorbed by the SVT is from MeV-scale electrons produced in the showers from lost-particles that interact in the beam pipe or the masks within the B1 magnets (see Figure 1). Since these electrons are minimum ionizing in silicon ( $dE/dx \simeq 90 \text{ keV}/300 \mu\text{m}$ ), the total dose rate depends on their number flux rather than their energy flux. The radial range of the secondary electrons is limited to a few centimeters by the detector’s 1.5 T field, which results in dose rates that fall off rapidly with distance from a showering material. This effect is responsible for the larger dose rates expected in the inner layers (proximity to the beam pipe), and for the

Table 2: Lost particle background simulation results for periods of stable colliding beams. The first two columns give the average and maximum dose rates expected for wafers in each layer. The last two columns give the average and maximum rates expected for hybrids in each layer. Dose rates are given over an operational year, defined as  $10^7$  seconds, so that  $1 \text{ mrad/s} = 10 \text{ krad/yr}$ . These results are different from those in Reference [3] since they are based on a more realistic vacuum pressure profile and the final SVT geometry.

SVT Layer	Avg Wafer Dose Rate	Max Wafer Dose Rate	Avg Hybrid Dose Rate	Max Hybrid Dose Rate
1	19 krad/yr	48 krad/yr	16 krad/yr	44 krad/yr
2	12 krad/yr	33 krad/yr	9.2 krad/yr	26 krad/yr
3	3.3 krad/yr	8.3 krad/yr	2.7 krad/yr	7.0 krad/yr
4	0.33 krad/yr	0.93 krad/yr	0.74 krad/yr	2.0 krad/yr
5	0.20 krad/yr	0.57 krad/yr	0.40 krad/yr	1.0 krad/yr

relatively larger dose rates in the hybrids of the outer two layers (proximity to the B1 magnets). Figure 8 shows the expected dose rates at the locations allocated for radiation sensors. The expected dose rate for 10mm wide (in  $r$ - $\phi$ ) sensors located in the horizontal plane (where rates are highest) is in the range of 80–130 krad per operational year ( $10^7$  seconds) or 8–13 mrad/s. The expected time structure of background levels during stable collisions will reflect operator tuning, and the ion-clearing gap (see Table 3).

During periods of PEP-II injection — either for initial filling or to top-off gradual losses — the dominant cause of beam loss is injection inefficiency. If a fraction  $f$  of the nominal full-current is injected and stored over an interval  $\Delta t$  and with an efficiency  $\epsilon$ , then the fractional rate of beam loss during the injection is  $(f/\Delta t) \cdot (1 - \epsilon)/\epsilon$ . The beam fraction injected during initial filling is  $f = 100\%$ , and during top-up is  $f = 1 - \exp(-\Delta t_{\text{inj}}/t_0)$  where  $\Delta t_{\text{inj}}$  is the time between top-ups, and  $t_0$  is the beam lifetime. Figure 5 shows the expected rate of injection losses assuming  $\epsilon = 75\%$ , with  $\Delta t = 6$  mins for initial filling and  $\Delta t = 3$  mins for top-up every hour ( $\Delta t_{\text{inj}} = 60$  mins). We also assume  $t_0 = 6.0$  hrs for the high-energy beam (HEB) and 2.7 hrs for the low-energy beam (LEB), which yield  $f = 15.4\%$  (HEB) and 31.0% (LEB) for

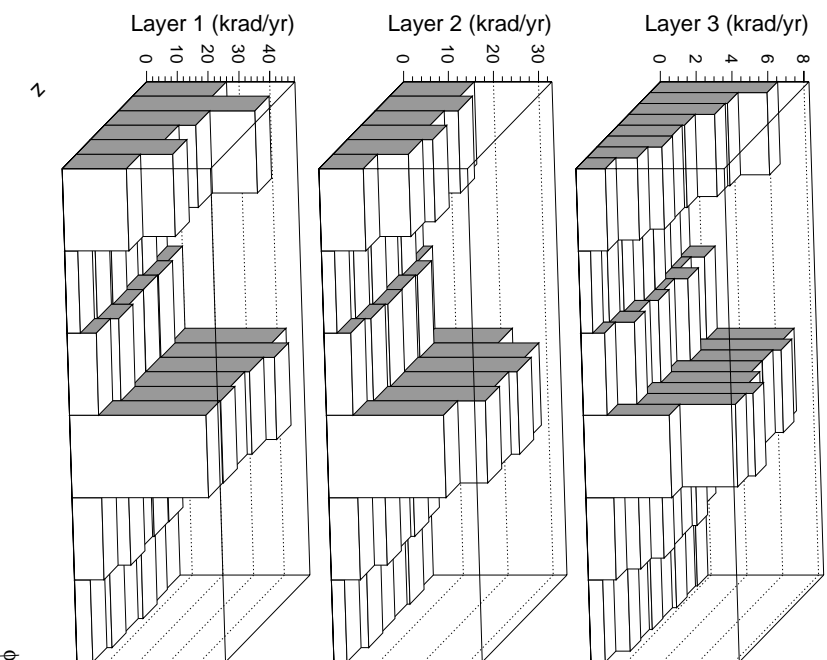


Figure 6: Lost particle background simulation results for periods of stable colliding beams. The three plots show the spatial distributions of absorbed dose predicted for the inner three layers of the SVT. Each histogram bin represents either a wafer or a hybrid: the hybrids are located at the ends (in  $z$ ) of each module, and the wafers are in between. Dose rates are given over an operational year, defined as  $10^7$  seconds, so that  $1 \text{ mrad/s} = 10 \text{ krad/yr}$ . These results differ from those in Reference [3] since they are based on more realistic vacuum pressure profiles and the final SVT geometry.

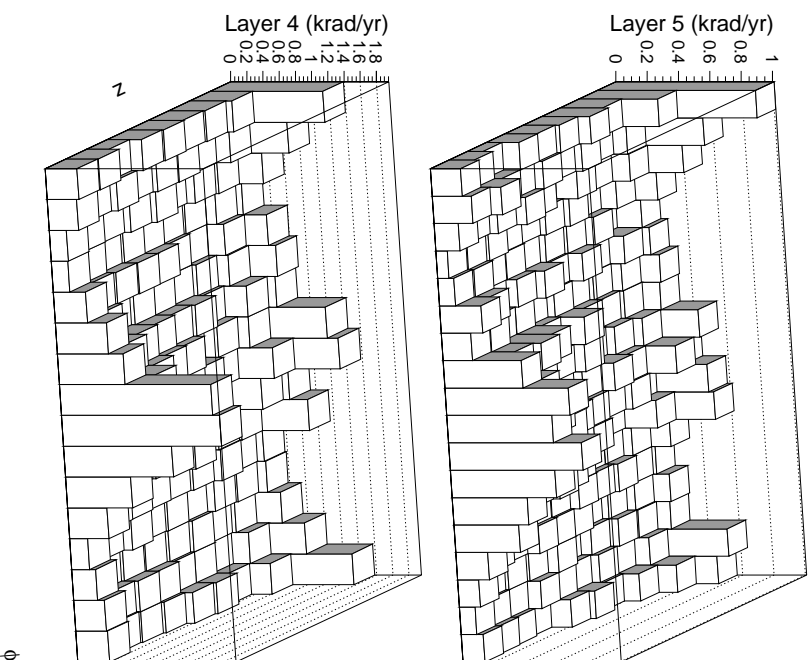


Figure 7: Lost particle background simulation results for periods of stable colliding beams. The two plots show the spatial distributions of absorbed dose predicted for the outer two layers of the SVT. Each histogram bin represents either a wafer or a hybrid: the hybrids are located at the ends (in  $z$ ) of each module, and the wafers are in between. Dose rates are given over an operational year, defined as  $10^7$  seconds, so that  $1 \text{ mrad/s} = 10 \text{ krad/yr}$ . These results differ from those in Reference [3] since they are based on more realistic vacuum pressure profiles and the final SVT geometry.

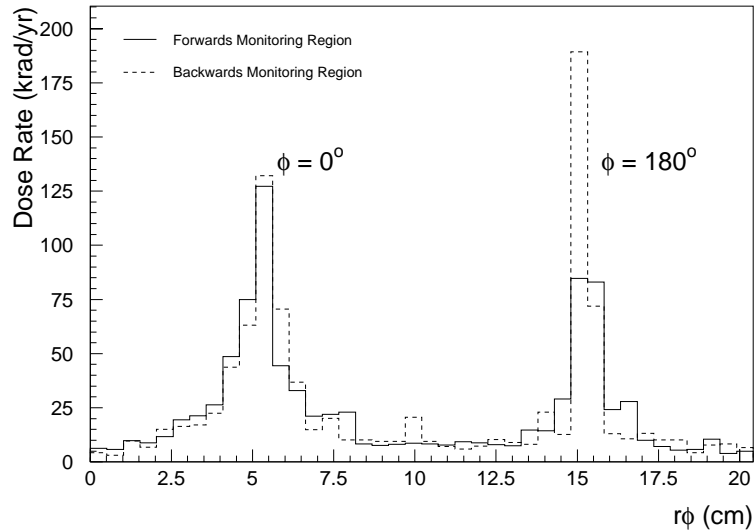


Figure 8: Lost particle background simulation results for periods of stable colliding beams. The plot shows the predicted dose rates at the small ends of the SVT support cones, where there is space allocated for radiation sensors. Each bin is approximately 5mm wide.

Table 3: Main timescales of PEP-II operation that are expected to be reflected in background rates.

Injection Damping Time	40 ms
Injection Period	16.7 ms
Beam revolution period	7.337 $\mu$ s
Ion-clearing gap width	370 ns
Bunch spacing	4.202 ns
Bunch width	33 ps

Table 4: Comparison of average beam-loss rates expected for each beam during different modes of accelerator operations. The rate for collisions is calculated as  $f/\Delta t_{\text{inj}}$ , where  $f$  is the beam fraction lost during  $\Delta t_{\text{inj}}$ . The factors given in parentheses are the ratios between injection and collision loss rates.

Operating Mode	Loss Rate (% of nom./min.)	
	HE Beam	LE Beam
Collisions	0.26%/min.	0.52%/min.
Filling	5.6%/min. ( $\times 22$ )	5.6%/min. ( $\times 11$ )
Top-up	1.7%/min. ( $\times 6.5$ )	3.4%/min. ( $\times 6.5$ )

topping-up.

Table 4 gives the numerical predictions corresponding to Figure 5. These values refer to the total losses around the ring. Since we do not expect that these losses are uniformly distributed around the ring, these values are probably not appropriate for the interaction region. However, we expect that the ratios between injection and collision losses are approximately valid since both of these losses are due to lost beam particles (due to different processes) hitting material near the interaction region. Note that this is an ad-hoc approximation that we adopt in the absence of any better model. Since we have not simulated injection backgrounds directly, we use the ratios in Table 4 to predict injection backgrounds. If we assume that the beams are dumped deliberately (i.e., without exposing the detector to any radiation) after 8 top-up cycles and then immediately refilled, then we expect that 30% of the detector background is due to injection losses. If the turn-around is reduced to one top-up cycle, the injection contribution increases to 51%. We expect that the time structure of background rates during injection will reflect the injection rate and the damping time (see Table 3).

The highest rates of beam loss (but hopefully not detector damage) occur when the stored beams are dumped. During a deliberate beam abort, the beam will be deflected by a kicker magnet and absorbed in a special purpose dump within 20  $\mu\text{s}$ [7], without increasing background levels near the

Table 5: Characteristic timescales for different beam accident scenarios.

Scenario	Time to lose beams
Beam-abort kicker failure	10 $\mu$ s
Klystron failure	100 $\mu$ s
Magnet failure	100 ms
Feedback system failure	1 s
Operator error	1 s

IR. Table 5 lists some possible accidental beam-loss scenarios with estimates of their characteristic timescales. For an order-of-magnitude estimate of the total dose that would be absorbed by SVT components during a beam accident that is not aborted, we scale the predicted dose absorbed during one minute of stable collisions by  $1/r$  where  $r$  is a typical average rate of beam loss during collisions. We use  $r = 0.4\%/min$ . (the average of the values in the first row of Table 4), obtaining  $1/r = 250$  minutes. Thus, we expect a total dose at the location allocated for radiation sensors (in the horizontal plane) of about 160 rad during an uncontrolled accidental beam dump (only a fraction of this dose would be received during a controlled beam abort). Note that this is an ad-hoc approximation with a large uncertainty, but that it is useful for setting the scale of the required system performance.

## 2.2 SVT Radiation Hardness

All SVT components located inside the support tube will be exposed to ionizing radiation during normal accelerator running. The components that are expected to be most vulnerable to radiation-induced damage are the detector wafers and the front-end readout chips. Other components inside the support tube, including the fanout and “tail” flex-circuits and the electronics on the hybrid (other than the readout chip) and matching-card, are not expected to be vulnerable.

The main radiation damage to the silicon wafers will consist of increased surface leakage current (up to  $1 \mu A/cm^2/Mrad$ ) and increased interstrip capacitance (5–15% after 1 Mrad with no further increase). The rate of this damage is expected to be greatest when bias is applied to the wafers. Type inversion can also occur at neutron fluences above  $10^{13}/cm^2$ , but we do not anticipate such large neutron backgrounds during normal BaBar running.

We do not expect any wafer damage to occur as a result of a small total dose received during a short time interval (instantaneous high dose rate).

The expected radiation damage to the readout chips consists of an accumulation of fixed charge at insulator-semiconductor interfaces, leading most noticeably to increased noise from the input transistor ( $\simeq 15\%$  after 0.5 Mrad,  $\simeq 30\%$  after 1.5 Mrad). The accumulation of fixed charge depends on the integrated radiation exposure of the readout chips, and not on the rate of this exposure. The rate of accumulation is expected to be greater when the chip is powered. A possible mechanism for damage at high dose rates is an electrical short between chip layers due to large numbers of electron-hole pairs being produced (“latchup”), and resulting in either transient or permanent damage to the chip.

The BaBar Technical Design Report[3] includes the requirement that the SVT meet its resolution specifications up to an integrated dose (from electrons and photons) that is 10 times the expected nominal dose, or 2 Mrad over 10 years for the first-layer wafers and electronics (based on the simulations described in Reference [3]). Simulations of the performance of SVT modules after irradiation are described in Reference [4]. The simulations include changes to wafer leakage currents and input transistor noise, and assume uniform exposure of each layer and its associated readout chips: 1.5 Mrad for layers 1–3, 0.5 Mrad for layer 4, and 0.25 Mrad for layer 5 (note that a uniform distribution is an approximation and that these values are conservative — see Section 2.1, above). The conclusion of these simulation studies is that layer 5 has the smallest signal-to-noise ratio after irradiation, because its larger size and longer integration time result in an increased noise per channel from surface leakage currents that outweighs the smaller doses expected at larger radii.

### 2.3 Interfaces with Other Systems

The SVT radiation-monitoring system will interact with several accelerator and detector systems, including the beam-abort system, the SVT power-supply system, and the detector and accelerator control systems. In most cases, we expect that the other systems involved will define their interfaces independently of radiation monitoring. Therefore, a requirement of this system is to conform to these interfaces. The requirements for the BaBar detector control system are described in Reference [5] and for the BaBar/PEP-II interface in Reference [6].

The PEP-II beam abort system is actually two independent systems: one for each beam. Each system consists of a trigger module, a set of kicker magnets, and a set of collimators. The trigger module[7] (“BATS”) will be a modified version of the SIAM2 module that accepts various types of trigger inputs and combines them in a logical-OR to trigger the main kicker magnet. The firing of the kicker magnet is synchronized to the next ion-clearing gap and causes the stored beam current to be dumped over one turn into a special-purpose collimator. The beam abort system is specified to be able to dump either beam within 20  $\mu$ s of receiving a trigger input. The trigger input from the SVT radiation monitoring system will consist of a high-to-low TTL transition applied through a standard coax cable into a 50 ohm load. The abort system is triggered by many sources, other than this system, which should detect the most likely accident scenarios independently of this system. Therefore, the SVT radiation monitor is not targeted at any particular failure mode but provides redundancy and protection against unexpected accidents.

Other accelerator systems that this system might interface with are the RF clock and the injection system. The RF clock could be used to derive timing signals that are synchronized to the revolution frequency of the beams, and will be accessible through a programmable CAMAC module (“PPDU”). An interface with the injection system could be used to alter dose-rate thresholds depending on whether injection is occurring, and to trigger limited-rate injection during periods of high injection losses.

The SVT power-supply system consists of 104 power supplies (one for each HDI module, providing detector bias and readout power) which can be independently controlled. The interfaces and detailed behavior of these modules have not yet been specified. However, it is expected that they will support independent interlock signals that trigger power-down and prevent subsequent power-up, and that there will be two modes of power-down: a normal slow ramp that can be performed regularly, and an emergency shutoff that is as fast as possible. These interlocks should be implemented according to the recommended standards for BaBar power-supply systems.

The detector and accelerator control systems will both be based on EPICS (or a similar package). The EPICS interface will be based on subroutines running under the VxWorks real-time operating system on VME single-board computers, and graphical user-interfaces running on Unix workstations. Since these are essentially software interfaces, their only requirement on this system is that it provide its data in a form accessible to a VME-based microprocessor. The EPICS interface should be designed according to

BaBar-wide guidelines.

## 2.4 Performance Requirements

We assume that this system uses radiation sensors located at the end of the support cones (see Figure 2), where the nominal dose rate during collisions is 8–13 mrad/s in the horizontal plane. We expect that SVT components can withstand short periods of high dose rate in which only a small total dose is received. In order to avoid unnecessary beam-aborts we require that this system not trigger during short bursts of radiation. Over longer periods, we require that SVT exposure be below about 10 times the expected nominal dose rates in order to limit the rate of long-term accumulated damage. We combine these two requirements by defining a damaging exposure for the SVT as a minimum dose absorbed at a minimum dose rate. Our primary performance requirement for this system is that it trigger the PEP-II beam-abort system when (and only when) avoidable damaging exposure is anticipated. We assume that the shortest interval over which an avoidable damaging exposure can occur is  $100 \mu\text{s}^1$  (see Table 3), and thus require that this system be able to respond to changes in the dose rate over this timescale.

We set the damaging dose threshold at 5% of the total nominal dose absorbed during an uncontrolled beam accident, or about 8 rad at the sensor location (horizontal dashed line in Figure 9). We set the damage dose-rate threshold at 10 times the nominal dose-rate during stable collisions, or about 100 mrad/s at the sensor location (diagonal dashed line in Figure 9). The corresponding region of damaging exposure is shown as the hatched region in Figure 9 in which exposure is parameterized in terms of dose received and the interval over which it is received. These thresholds for damaging exposure provide a worst-case upper limit on the thresholds used to trigger the beam-abort system. The actual trigger thresholds will be somewhere between these damaging levels and the nominal operating radiation levels, and will be determined based on operational experience. We require that this system be flexible enough to accommodate this range of possible thresholds.

In addition to protecting against SVT damage, we require that this system be sensitive to nominal conditions during stable collisions (10 mrad/s at the sensor location, indicated by the solid line in Figure 9) in order to provide

---

<sup>1</sup>A beam-abort kicker failure could cause damage in a shorter interval but we consider this to be unavoidable.

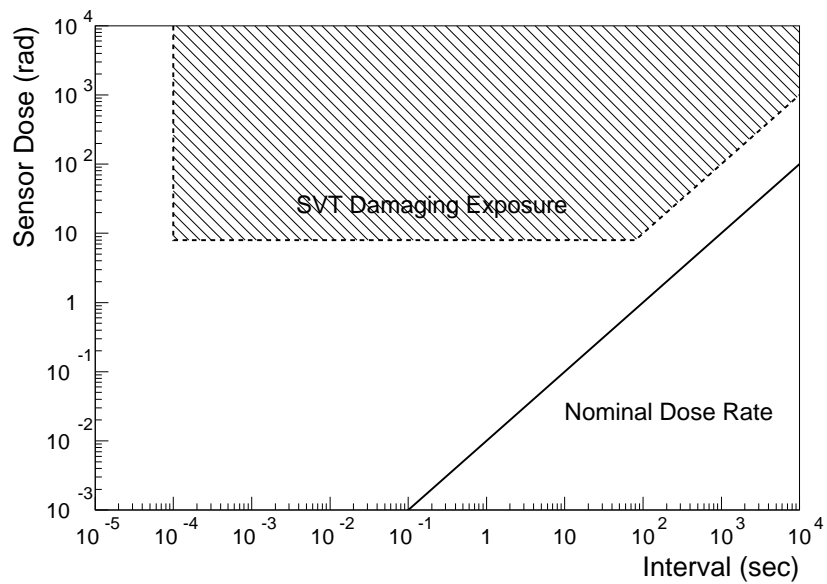


Figure 9: Plot of radiation exposure for a sensor located at the small end of the forward support cone, in the horizontal plane. Exposure is parameterized in terms of dose received and the interval over which it is received. The diagonal solid line shows the nominal dose rate expected at the sensor location. The hatched area shows the region we define as damaging exposure for the SVT.

data for the accelerator and detector control systems. Samples should be provided at a rate of about 2 Hz[5], and should have an accuracy of at least 10%. We also require that the integrated dose be accumulated with an accuracy of at least 10% over time scales in the range of 1 minute to 10 years. Taking the sum of all samples over a period provides a straightforward method to estimate integrated dose but requires careful control of systematic uncertainties.

### 3 Position Monitoring

The primary requirement of this system is to monitor the relative motions between the B1 magnets and the SVT, in order to ensure that no load is applied to the SVT. This system should be operational during mounting and unmounting of the SVT on the B1 magnets, during installation of the SVT in the support tube, during transportation of the support tube from the assembly lab to the interaction region, during installation and removal of the support tube in the detector, and when the support tube is inside the detector. Therefore, a requirement of the monitoring system is that it have a portable readout system which can be used during installation of the SVT and transportation of the support tube.

The SVT cones are connected to the B1 magnets via a gimbal system in both the forward and backward regions, as shown in Figure 10. The gimbals allow rotation of the cones relative to the B1 magnets about any axis passing through the center of the gimbal and lying in a plane perpendicular to the central axis of the magnet. In addition to these sorts of rotations, the backward gimbal allows relative motion of  $\pm 2$  mm in  $z$  and unrestricted rotation about the  $z$  axis. The B1 magnets are mounted to the Q1 magnets and the Q1 magnets are mounted to the inside of the stainless steel sections of the support tube. Each end of the central beampipe is connected through bellows to the beampipe sections in the B1 magnets. Therefore, relative motion of the two B1 magnets is constrained through their mounts to the Q1 magnets and support tube, not through the beampipe. Once the two B1 magnets are mounted inside the support tube, no relative motion in  $z$  or  $\phi$  is expected.

The maximum relative motion of the forward SVT support cone with respect to the forward B1 magnet is a rotation of  $2.25^\circ$  (39 mrad), determined by when the inner surface of the support cone and outer surface of the B1

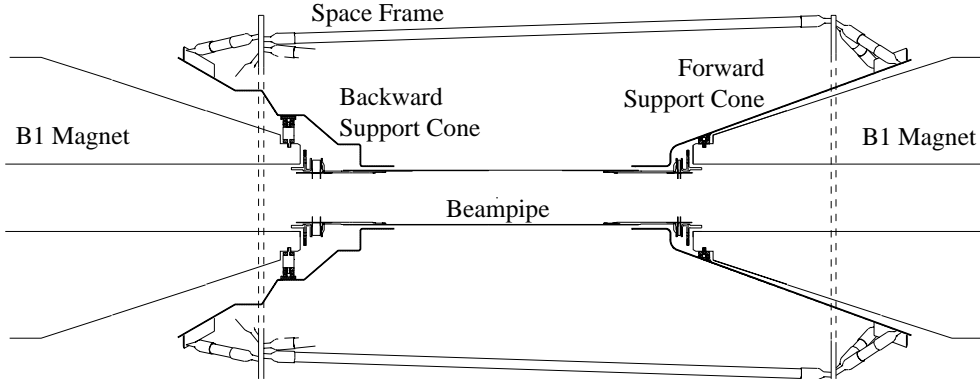


Figure 10: Cross-section ( $y$ - $z$ ) of the PEP-II interaction region showing the kinematic mounting of the SVT support cones from the B1 magnets using gimbal rings. The two support cones are rigidly connected to each other by a space frame (shown at large radius) and by the ribs supporting each detector module (not shown).

magnet first make contact as shown in Figure 11. During this rotation, the minimum gap between the large end of the cone and the B1 magnet changes from the nominal 9.8 mm to 0 mm, while the minimum gap between the small end of the cone and the beampipe changes from the nominal 3.7 mm to 2.7 mm. Therefore, the forward cone will always touch the B1 magnet at the large end of the cone first. The total range of possible gap sizes at this point is 0 to 2 cm.

In the backward region, the gap between the large end of the cone and the B1 magnet is much larger (about 5 cm). Service lines for the interaction region will run between the backward cone and the B1 at certain locations in azimuth. However, there will be room for a standoff or spacer to be attached to the B1 magnet to decrease the gap to approximately 5 mm to ensure that contact will occur at this point first.

The SVT support cones are each constructed in two parts and joined in the vertical plane. There need to be enough position sensors to monitor each half of the SVT “clamshell” separately during installation onto the B1 magnets.

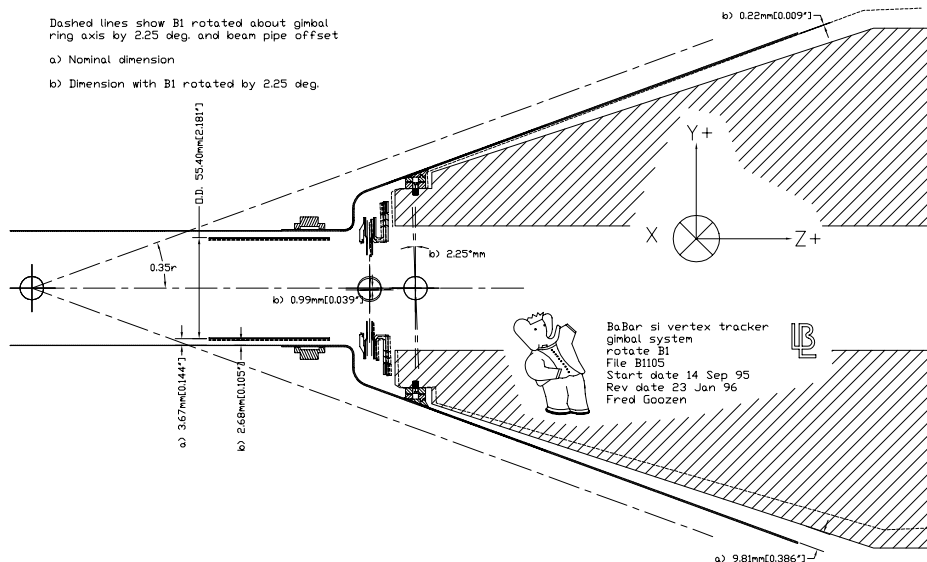


Figure 11: Cross-section through the forward end ( $z > 0$ ) of the interaction region showing the forward B1 magnet in its nominal position relative to the support cone (solid lines) and rotated by  $2.25^\circ$  (dashed lines) when it first makes contact with the support cone at the cone's large end.

The deflection of the support tube when loaded and simply supported at the ends is expected to be 1.5–2.4 mm, depending on the exact design of the carbon-fiber section. A deflection of 2.0 mm would result in a 1.1 mrad ( $0.05^\circ$ ) relative rotation of the SVT cones with respect to the B1 magnets, resulting in a change of 0.3 mm in the gap at the large end of the cones. However, the plan is to align the magnetic components along a straight line, predeflect the support tube with appropriate loads before installing the components, and then install the support tube around the components with a final configuration in which the support tube sags but the machine elements are still aligned. The position monitors must measure the gap between the cones and the B1 at all times during this process. The support tube motion expected during a “standard” earthquake defined for BaBar engineering is about  $\pm 2.1$  mrad, or twice that due to support tube sag.

The position monitoring system should measure expected deflections with an accuracy of (5–10)% and measure gaps where contact can be made with an accuracy of at least 1% of the nominal gap. Since the expected deflections are in the range of a few hundred microns, a precision of approximately 10  $\mu\text{m}$  is desirable. The nominal gap at the location where contact is first made (at the outer radius of the support cone) is 1 cm. Therefore the requirement on the precision with which we measure the gap is about 100  $\mu\text{m}$ . The accuracy with which the gap is measured should also be 100  $\mu\text{m}$  or better, especially at small gap sizes (about 1 mm) when the cone and B1 are about to touch.

A secondary goal for the position monitoring system is to provide input for determining the alignment of the SVT with respect to the drift chamber. To achieve this, the gap between the inner radius of the drift chamber endplates and the outer stainless steel wall of the support tube will be monitored. This gap is nominally 1 cm but can range from 0.5 to 1.5 cm as the support tube is moved to tune PEP-II. Relative motion in  $z$  and  $\phi$  will also be monitored at this location. The inside surfaces of the drift chamber endplates are located at  $z = +174.9$  cm in the forward direction and  $z = -101.5$  cm in the backward direction.

The positions of machine components in the interaction region will be monitored by the accelerator group with respect to a set of stretched wires. One wire will pass through the entire support tube, with its ends mounted from the rafts outside the support tube. The current plan is to measure the gap between this wire and the support tube walls, the B1 magnets and the Q1 magnets, each at several locations. The details of this system are currently being worked out by an alignment engineer in the PEP-II group. In principle, information from these three systems can be combined to provide information relevant for the alignment of the tracking systems.

The requirement on the relative alignment of the drift chamber and SVT is primarily determined by degradation in tracking resolution that results from a misalignment. The greatest impact is on high momentum tracks for which both the drift chamber and SVT contribute to momentum resolution since multiple scattering in material between the two systems is not as significant. A study was done by Eric Soderstrom and Art Snyder that showed that the mass resolution for  $B^0 \rightarrow \pi^+\pi^-$  is degraded for relative SVT/drift-chamber misalignments of greater than  $\simeq 50$   $\mu\text{m}$ . Under the assumption that the support tube and the B1 and Q1 magnets can be treated as a single rigid object, a measurement of motion of the support tube with respect to the drift chamber in  $x$ ,  $y$ ,  $z$  or  $\phi$  translates directly into a measurement of motion of

the SVT with respect to the drift chamber. Sensitivity to rotations of the central axis of the support tube (and hence the SVT) with respect to the central axis of the drift chamber can be monitored with sensors at both ends of the drift chamber. The sensitivity to these sorts of rotations is enhanced by the large distance between the drift chamber endplates. Therefore, to know the relative alignment of the SVT and drift chamber to better than  $50\ \mu\text{m}$ , the precision with which the relative position of the drift chamber and support tube is measured should be better than  $50\ \mu\text{m}$ . In addition, to check the assumption that the support tube and the B1 and Q1 magnets can be treated as a single rigid object, the position of the magnets with respect to the support tube must also be monitored with a precision of better than  $50\ \mu\text{m}$ .

Ultimately, the alignment of the SVT and drift chamber will be determined with high-momentum charged tracks passing through both devices. Approximately 2000 tracks are required to reach a precision of  $50\ \mu\text{m}$  on the relative SVT/drift chamber alignment [8]. Assuming two useful high-momentum tracks per event, this corresponds to 1000 events. Therefore, at design luminosity, global alignment constants can be recalculated with data accumulated in about 5 minutes. However, at startup the luminosity could be significantly lower. With 10% of design luminosity, the time required to accumulate data for a global alignment is about one hour. The position monitoring systems will be most useful at startup when luminosity is low, for identifying the types of motion to which the alignment algorithm must be sensitive, and for detecting sudden changes in alignment.

## 4 Temperature Monitoring

The temperatures of three components of the SVT system must be monitored: the water-cooled HDI's on which the frontend readout electronics are located, the mechanical structure supporting the SVT, and any temperature-sensitive sensors. Where feasible, SVT temperature monitoring should follow BaBar-wide guidelines for sensors and readout electronics.

### 4.1 Mechanical Structure

Stable temperatures for the detectors and support structures are needed so that we can meet the requirement that the relative positions of the various

wafers be stable to the  $5\ \mu\text{m}$  level over long periods of time (months or more). On p. 143 of the TDR, the following statements are made: “Preliminary calculations for the thermal expansion of the entire structure predict on the order of  $0.5\ \mu\text{m}/^\circ\text{C}$  over the length of the active region of the detector. If the temperature inside the support tube is maintained at  $\pm 1^\circ\text{C}$ , thermal expansion will not be a problem.” Therefore, temperature monitors with an accuracy of about  $1^\circ\text{C}$  maintained over a period of months and a precision of about  $0.5^\circ\text{C}$  located on the mechanical structure itself (say the space frame) will satisfy the monitoring requirements for thermal expansion.

The local alignment of SVT wafers will be done with high-momentum charged tracks. The number of hadronic events needed to do a local alignment has been estimated [8] to be about 77,000 for the outer layer; the inner layers require fewer. At design luminosity, it will take about 7 hours to accumulate this much data. In early PEP-II running, it will take much longer. Therefore, we must be able to monitor temperature changes that can cause wafers to move with respect to each other and that have a shorter timescale than the alignment cycle.

These temperature monitors should be located near the humidity monitors (described below) so that they also provide a temperature measurement needed to calculate the dew point from the measured relative humidity.

## 4.2 HDI’s

The temperature monitors on the HDI’s in the vicinity of the frontend electronics must provide a fail-safe interlock on the power supplies for the readout electronics. The frontend electronics generate about 3 mW per channel, or about 500 W for the 150,000 readout channels. The electronics is actively cooled with water and should be shut down if for any reason the temperature rises significantly above the normal operating range. There will be one resistive temperature monitor per HDI. The monitor must fit in an area on the HDI approximately  $1\ \text{mm} \times 2\ \text{mm}$ .

The gain and shaping time of the SVT electronics are sensitive to temperature. However, SPICE simulations have shown that this sensitivity is not an issue for temperatures in the range  $(30 - 50)^\circ\text{C}$ .

The temperature monitors on the HDI and flow monitors for the cooling system should be part of the power-supply interlock system for the SVT readout electronics, so that the power to the electronics cannot be turned on until flow is established and the power to the electronics will be turned off if

the temperature rises above a threshold value.

### 4.3 Temperature-dependent Sensors

Any sensors located near the beampipe (e.g., radiation monitors) will be in an environment with a temperature distribution that is not uniform in space or time. Therefore, sensors (such as photodiodes) that have temperature-dependent characteristics must be instrumented with temperature monitors. Radiation-monitoring sensors will be mounted at the small ends of the SVT support cones. Their temperature will be influenced by the nearby electronics mounted on the HDI's for layers 1 and 2, the cooling ring for the layer 1 and 2 HDI's, and the B1 magnet. The temperature of the water in the HDI cooling rings will be about 10°C at the inlet and about 2°C higher at the outlet. The water enters at the bottom and exits at the top of each half-ring. The HDI substrate (AlN) will be at 12°C and the electronic readout chips at 30°C. The temperature of the B1 magnets will be 20°C and must be stable to  $\pm 1^\circ\text{C}$ . The temperature at the location of any sensors near the beampipe can be expected to change depending on whether the SVT electronics are powered and whether the HDI cooling water is flowing.

## 5 Humidity Monitoring

The purpose of monitoring humidity is to determine when there is sufficient moisture in the environment around the SVT detectors and electronics to condense on surfaces. In particular, we need to determine the temperature at which the moisture would condense. This temperature must always be lower than the coldest surface in the vicinity of the SVT detectors or readout electronics, which will usually be the inlet water cooling lines.

There are at least three different quantities that one can measure: absolute humidity, relative humidity and dew-point temperature. The absolute humidity is a measure of the moisture content in the atmosphere. The relative humidity is the absolute humidity divided by the moisture content at saturation at that temperature. In order to use a measurement of relative humidity, one must also know the temperature of the gas. The dew-point temperature is the temperature at which condensation of moisture would begin if the gas were cooled at constant pressure. We must ensure that the dew-point temperature of the gas near the SVT electronics and detectors is

significantly below the temperature of the electronics and detectors.

To prevent condensation, the incoming cooling lines will be insulated. In addition, the region near the interaction point will be purged with a continuous flow of dry nitrogen. If the dew-point temperature approaches the temperature of the cooling lines, action must be taken to either increase the purge rate with dry nitrogen, raise the temperature, or both.

Because of space constraints, the monitors must be very compact. This requirement restricts us to relative humidity monitors which require, in addition, a temperature measurement in the vicinity of the relative humidity measurement. Where feasible, SVT humidity monitoring should follow BaBar-wide guidelines for sensors and readout electronics.

## 6 Schedule

Table 6 summarizes the main schedule constraints on the development of SVT monitoring systems. In the spring of 1997, PEP-II will begin commissioning the high-energy ring and we plan to have a prototype radiation monitoring system ready at that time for studying backgrounds at the interaction region (IR). We expect that the sensors and readout electronics for this prototype system will closely resemble those of the final system for BaBar, but that the mechanical support and the number of sensors will be quite different. Before the installation of the final IR in PEP-II early in 1998, mechanical tests of the complete support-tube assembly are planned which will include the SVT mechanical structure. We plan to monitor the relative positions of the SVT support cones with respect to the B1 magnets during these tests using the same sensors as for the final BaBar position-monitoring system, and a standalone readout that will also be used during the final support-tube installation into BaBar.

All monitoring components to be installed on the support cones or HDIs must be available before final assembly of the SVT detector modules onto the support cones begins in July 1998. The final deadline for complete integration of all monitoring systems into the SVT is December 1998, when detector cosmic-ray tests are scheduled to begin.

Table 6: Schedule constraints on the development of SVT monitoring systems.

Apr 1997	—	radiation-monitoring prototype for PEP-II commissioning
Early 1998	—	position-monitoring prototype for SVT/IR mechanical tests
July 1998	—	delivery of all final monitoring components for final SVT assembly
Dec 1998	—	final integration of all SVT monitoring for BaBar cosmic-ray tests

## References

- [1] BaBar SVT Group, “BaBar SVT Electronics Requirements”, BaBar Note 306 (1996).
- [2] BaBar SVT Group, “BaBar SVT Mechanical Systems Design Requirements”, BaBar Note 298 (1996).
- [3] BaBar Collaboration, BaBar Technical Design Report, SLAC-R-95-457 (1995).
- [4] Wladek Dabrowski and Robert Johnson, “Simulations of the Performance of the Proposed BaBar SVT Modules”, BaBar Note 263 (1995).
- [5] Gerry Abrams et al., “BaBar Detector Controls System Requirements Document”, in preparation (see <http://www.slac.stanford.edu/BFROOT/doc/Computing/Online/Reports/systemReq.ps> for the latest draft).
- [6] Gerry Abrams et al., “BaBar and PEP-II: Interface Requirements”, in preparation (see <http://www.slac.stanford.edu/BFROOT/doc/Computing/Online/Reviews/Feb.96/PepII-Iface-Reqs.ps> for the latest draft).
- [7] R. Champion, “PEP-II Beam-Abort Trigger System Design Specification”, SLAC Design Specification (1996).

- [8] David Brown, “BaBar VDET Alignment Requirements”, BaBar Note 148 (1995).